

## Necklace-like Hollow Carbon Nanospheres from the Pentagon-Including Reactants: Synthesis and Electrochemical Properties

Changzheng Wu, Xi Zhu, Lila Ye, Chuanzi OuYang, Shuangquan Hu, Lanyu Lei, and Yi Xie\*

*Nano-materials and Nano-chemistry, Hefei National Laboratory for Physical Sciences at Microscale, University of Science & Technology of China, Hefei, Anhui 230026, China*

Received May 15, 2006

Necklace-like hollow carbon nanospheres (CNSs) have been successfully synthesized from the pentagon-including reactants, which provide an auxiliary example for the theoretical prediction that necklace-like hollow CNSs are assumed to be composed of the regular occurrence of nonhexagonal rings at the atomic level. Benefits of the as-obtained hollow CNSs also arise from the high Brunauer–Emmett–Teller value of 594.32 m<sup>2</sup>/g and a narrow pore distribution at 5 nm. The electrochemical hydrogen storage experiments for the as-obtained necklace-like hollow CNSs exhibit a capacity of 242 mAh/g at the current density of 200 mA/g, corresponding to a hydrogen storage of 0.89 wt %, which is higher than the previously reported electrochemical capacities for the multiwalled carbon nanotubes (MWCNTs). Furthermore, the as-obtained necklace-like hollow CNSs show a lithium capacity advantage compared with the carbon solid particles for application in lithium batteries. These results indicate that the necklace-like hollow CNSs provide a new candidate for the application in hydrogen storage and lithium batteries.

### 1. Introduction

Pentagon, as a kind of nonhexagonal defect existing in the seamless hexagonal network, plays a vital role in the formation of various carbon nanostructures (CNSs). For example, according to structural analysis, the smallest carbon cage of a C<sub>60</sub> molecule can be constructed from 12 pentagons in the form of a fulvalene unit.<sup>1</sup> As reported, pentagons are also certainly present in nanohorns,<sup>2</sup> carbon onions,<sup>3</sup> and nanotube caps.<sup>4</sup> As for the hollow carbon spheres, to date, the well-accepted opinion for the formation of hollow carbon spheres is ascribed to the rolling of a hexagonal lattice of sp<sup>2</sup>-bonded graphite sheets, neglecting the action of nonhexagonal defects in the formation process.<sup>5</sup> However, hollow CNSs can be regarded as a combination of two multiwalled nanotube caps, and then the pentagon unit ought to be present in the hollow carbon spheres as those in nanotube caps. In this regard, the pentagon units are necessary for the construction of hollow carbon spheres and

may provide further possibilities for new carbon architectures.<sup>6</sup>

Herein, we demonstrate that necklace-like hollow CNSs can be achieved from two pentagon-including reactants of ferrocene [Fe(C<sub>5</sub>H<sub>5</sub>)<sub>2</sub>] and hexachlorocyclopentadiene (C<sub>5</sub>Cl<sub>6</sub>), verified that the pentagon defects do influence the formation of necklace-like hollow CNSs, and provided an auxiliary example for the theory prediction that necklace-like hollow CNSs are assumed to be composed of the regular occurrence of nonhexagonal rings at the atomic level.<sup>7</sup>

Nanosized carbon materials have received considerable interest for the development of a new generation of hydrogen storage materials because of their unique characteristics such as high surface reactivity and strong gas adsorption.<sup>8</sup> As is known, multiwalled carbon nanotubes (MWCNTs) can be regarded as an ideal pore structure fit for hydrogen storage and exhibit a good electrochemical hydrogen storage performance and an improvement in the cycle performance elsewhere.<sup>9</sup> For example, electrochemical hydrogen storage for the MWCNTs has been investigated extensively: Nütze-

\* To whom correspondence should be addressed. E-mail: yxie@ustc.edu.cn. Tel: 86-551-3603987. Fax: 86-551-3603987.

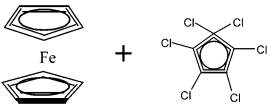
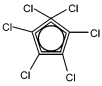
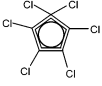
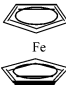
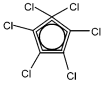
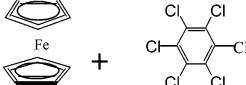
(1) Manolopoulos, D. E. *Chem. Phys. Lett.* **1992**, *192*, 330–332.  
 (2) Iijima, S.; Yudasaka, M.; Yamada, R.; Bandow, S.; Suenaga, K.; Kokai, F.; Takahashi, K. *Chem. Phys. Lett.* **1999**, *309*, 165–170.  
 (3) Kroto, H. W.; McKay, K. *Nature* **1988**, *331*, 328–331.  
 (4) Iijima, S.; Ichihashi, T.; Ando, Y. *Nature* **1992**, *356*, 776–778.  
 (5) (a) Liu, J. W.; Shao, M. W.; Tang, Q.; Chen, X. Y.; Liu, Z. P.; Qian, Y. T. *Carbon* **2003**, *41*, 1682–1685. (b) Hu, G.; Ma, D.; Cheng, M.; Liu, L.; Bao, X. H. *Chem. Commun.* **2002**, *17*, 1948–1949.

(6) Lee, C. Y.; Chiu, H. T.; Peng, C. W.; Yen, M. Y.; Chang, Y. H.; Liu, C. S. *Adv. Mater.* **2001**, *13*, 1105.

(7) Terrones, H.; Terrones, M.; Hernandez, E.; Grobert, N.; Charlier, J. C.; Ajayan, P. M. *Phys. Rev. Lett.* **2000**, *84*, 1716–1719.

(8) Conway, B. E. *Electrochemical supercapacitors: scientific fundamentals and technological applications*; Kluwer Academic/Plenum: New York, 1999.

**Table 1.** Summary Information for the As-Obtained Carbon Materials by Different Reactants at Different Temperatures

Reactants	Reaction Temperature	Morphology
	350 °C	~~~~~
	500 °C	Necklace-like hollow Carbon nanospheres
	600 °C	Hollow vessels
Mg + 	500 °C	
K + 	500 °C	Chain-like carbon solid spheres
	500 °C	Carbon solid particles
	500 °C	Carbon solid particles
	500 °C	Lamellar sheets

nadel et al. first made the electrode of the MWCNT sample together with catalyst Fe and Ni synthesized by an arc-discharge method under proper pressure, which displayed the electrochemical hydrogen storage capacity of 110 mAh/g at the charge/discharge current density of 200 mA/g.<sup>10</sup> Qin et al. have made the MWCNTs/Ni electrode at the mass ratio of 1:10 in which the diameters of the MWCNTs synthesized by chemical vapor deposition are 30–60 nm and the capacity is 200 mAh/g at the charge/discharge current density of 200 mA/g based on the following electrochemical reaction mechanism:<sup>11</sup>



In this regard, hollow carbon spheres usually possess a thin wall and a hollow inside and also have the potential of providing an ideal pore structure fit for hydrogen storage and should exhibit a good electrochemical hydrogen storage performance and a cycle performance similar to that of the MWCNTs. However, the electrochemical hydrogen storage performance of hollow carbon spheres (as one kind of

morphology catalog) was lacking possibly because of the difficulty in the large-scale synthesis of hollow CNSs so far. Then, the large-scale synthesis of hollow CNSs in the present work provides an example for investigating their electrochemical hydrogen storage performance for hollow carbon spheres, which is apparently much needed from both technical and scientific points of view. Herein, the electrochemical hydrogen storage experiments for the as-obtained necklace-like hollow CNSs with high Brunauer–Emmett–Teller (BET) values exhibit a capacity of 242 mAh/g at a current density of 200 mA/g, corresponding to a hydrogen storage of 0.89 wt %, which is higher than the previously reported electrochemical capacities for the MWCNTs.<sup>10,11</sup> Also, the as-obtained necklace-like hollow CNSs exhibit a lithium storage capacity advantage compared with carbon solid particles for application in lithium batteries.

## 2. Experimental Section

In a typical procedure, under an argon gas atmosphere,  $\text{Fe}(\text{C}_5\text{H}_5)_2$  (1 mmol) and  $\text{C}_5\text{Cl}_6$  (2 mmol) were loaded into a quartz tube of 20-mL capacity, which was then put into a 65-mL stainless steel autoclave. Note that the 20-mL quartz tube was protected under an argon gas atmosphere. After the autoclave was sealed and put into an electronic furnace, its temperature was increased to 500 °C in 60 min, maintained at 500 °C for 4 h, and then cooled to room temperature naturally. The product was filtered and washed with dilute HCl, distilled water, and toluene to remove the possible impurities. Finally, the as-synthesized products were dried under vacuum at 60 °C for 3 h. All of the comparison experiments were carried out in similar procedures, except the replacement of different reactants as shown in Table 1.

- (9) (a) Dillion, A. C.; Jones, K. M.; Kiang, T. A.; Bethune, C. H.; Heben, M. J. *Nature* **1997**, *386*, 377. (b) Dai, G. P.; Liu, C.; Liu, M.; Wang, M. Z.; Cheng, H. M. *Nano Lett.* **2002**, *2*, 503. (c) Zhang, H. Y.; Fu, X. J.; Yin, J. F.; Zhou, C.; Chen, Y. M.; Li, M. H.; Wei, A. X. *Phys. Lett. A* **2005**, *339*, 370.
- (10) Nützenadel, C.; Züttel, A.; Chartouni, D. *Electrochem. Solid-State Lett.* **1999**, *2*, 30–32.
- (11) Qin, X.; Cao, X. P.; Liu, H.; Yuan, H. T.; Yan, D. Y.; Gong, W. L.; Song, D. Y. *Electrochem. Solid-State Lett.* **2000**, *3*, 532–535.

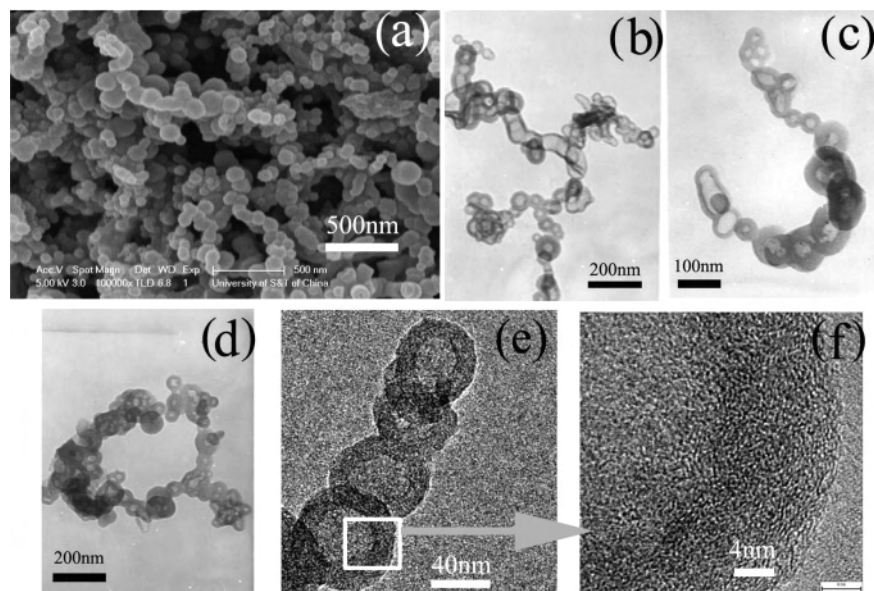


**Figure 1.** FE-SEM image (a) and TEM images (b–e) of the products for the as-obtained necklace-like hollow CNSs by the reaction of ferrocene [ $\text{Fe}(\text{C}_5\text{H}_5)_2$ ] and hexachlorocyclopentadiene ( $\text{C}_5\text{Cl}_6$ ) at  $500^\circ\text{C}$ , where the as-obtained hollow carbon spheres curve smoothly and entangle together to form the Y, C, Q, and linear shapes (Figure 2b–e). Shown in part f is the HRTEM image for the hollow spheres part.

Raman spectra were recorded at room temperature with a LABRAM-HR Confocal Laser MicroRaman spectrometer. The field emission scanning electron microscopy (FE-SEM) images were taken on a JEOL JSM-6700F scanning electron microscope. The transmission electron microscopy (TEM) images were performed with a Hitachi model H-800 instrument with a tungsten filament, using an accelerating voltage of 200 kV. High-resolution TEM (HRTEM) images were carried out on a JEOL-2010 transmission electron microscope at an acceleration voltage of 200 kV. Elemental analysis was taken on an Elementar Vario EL-III elemental analysis instrument.

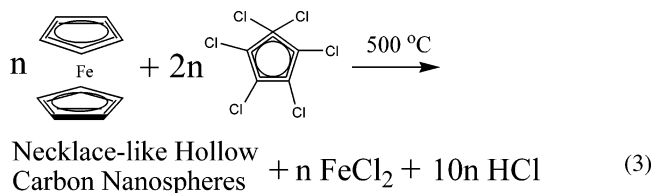
Electrochemical measurements of necklace-like hollow CNSs were performed using  $\text{Ni}(\text{OH})_2/\text{NiOOH}$  as the counter electrode and  $\text{Hg}/\text{HgO}$  as the reference electrode in a 6 N KOH electrolyte at room temperature under a normal atmosphere (1 bar). The hollow carbon sphere electrodes were prepared as follows: a composite of 20 mg of purified hollow carbon spheres and 60 mg of copper powders was filled in a porous nickel substrate. The hollow carbon sphere electrode was charged for 2 h at a current density of 200 mA/g and discharged at the same current density after a 5-min rest. The cutoff voltage is  $-0.4$  V (vs  $\text{Hg}/\text{HgO}$ ). The charge/discharge current density was controlled at 50 mA/g except for special illumination. All of the electrochemical hydrogen storage experiments were carried out using the Land battery system (CT2001A).

The performance of the sample as a cathode was evaluated using a Teflon cell with a lithium metal anode. The cathode was a mixture of necklace-like hollow CNSs/poly(vinylidene fluoride) with a weight ratio of 9:1. The electrolyte was 1 M  $\text{LiPF}_6$  in a 1:1 mixture of ethylene carbonate/diethyl carbonate, and the separator was Celgard 2320. The cell was assembled in a glovebox filled with highly pure argon gas ( $\text{O}_2$  and  $\text{H}_2\text{O}$  levels < 5 ppm). The galvanostatic charge/discharge experiment was performed between 2.0 and 0.05 V at a constant discharge rate of 0.2 mA/cm<sup>2</sup>. All of the lithium ion battery electrode experiments were carried out using the Land battery system (CT2001A).

### 3. Results and Discussion

**3.1. Morphologies of the As-Obtained Products.** The whole reaction between the two pentagon-including reactants

of ferrocene [ $\text{Fe}(\text{C}_5\text{H}_5)_2$ ] and hexachlorocyclopentadiene ( $\text{C}_5\text{Cl}_6$ ) could be illustrated as follows:



Reaction (3) results in the large-scale necklace-like hollow CNSs revealed by FE-SEM, in which the proportion of hollow spheres in the sample is 80–85% (Figure 1a,b). The TEM images of these hollow CNSs show the hollow nature on the basis of a strong contrast between the dark edge and pale center.<sup>12</sup> It is found that necklace-like hollow CNSs are up to several micrometers long, with the outer diameters in the range of 50–100 nm and the average thickness of the well-defined wall less than 10 nm. The as-obtained hollow carbon spheres curve smoothly and entangle together to form the Y and C shapes (Figure 1b,c). More interestingly, the tens of spherical units link from the end of the necklace to its head to form the closed circle, as shown in Figure 1d. The relatively straight necklace is also found in Figure 1e. The typical HRTEM performed on one sphere in the necklace in Figure 1f also reveals the contrast between the dark edge and pale center and the poor crystallinity, further confirming the hollow nature of the products and its low degree of long-range order resulting from the pentagons, respectively. Additionally, the X-ray photoelectron spectroscopy (XPS) survey spectrum (S1 in the Supporting Information) for the as-obtained hollow CNSs shows that no obvious Fe and Cl could be detected in the samples, indicating that the level of Fe and Cl is lower than the resolution limit of XPS (1 atom %).

(12) Tenne, R., Karlin, K. D., Eds. *Progress in Inorganic Chemistry*; John Wiley & Sons: New York, 2002; Vol. 50, pp 269–315.

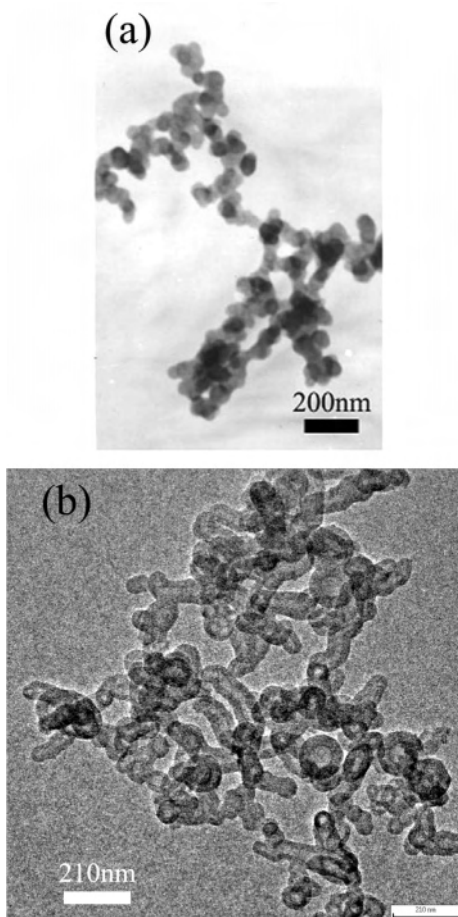


**Figure 2.** TEM images of (a) the solid chainlike carbon spheres by the reaction of two pentagon-including reactants of naphthalene ( $C_{10}H_8$ ) and hexachlorobenzene ( $C_6Cl_6$ ) and (b) the carbon vessels by the reaction of ferrocene [ $Fe(C_5H_5)_2$ ] and hexachlorocyclopentadiene ( $C_5Cl_6$ ) at 600 °C, where the vessels were the main products.

**3.2. X-ray Diffraction (XRD) and Raman Investigation of the Disordering Nature and Amorphism of As-Obtained Necklace-Like Hollow CNSs.** For comparison, solid chainlike carbon spheres were prepared by the reaction of two hexagonal units such as  $C_6Cl_6$  and  $C_{10}H_8$  under the same conditions. TEM images as shown in Figure 2 displayed the solid chainlike spheres with the average diameters of 60–90 nm and lengths of several micrometers. XRD and Raman spectra clearly indicated the difference between the necklace-like hollow CNSs and the as-obtained solid chainlike carbon spheres.

As expected, using the pentagon units as reactants in this case would certainly lead to the existence of a certain amount of pentagons, which will increase the disorder degree in the graphitic carbon.<sup>13</sup> Raman spectroscopy has been used to investigate the vibrational properties of the carbon structures, which also allow us to draw further conclusions about the information on the degree of long-range order and the bonding topology for carbon atoms.<sup>14</sup> In this work, Raman

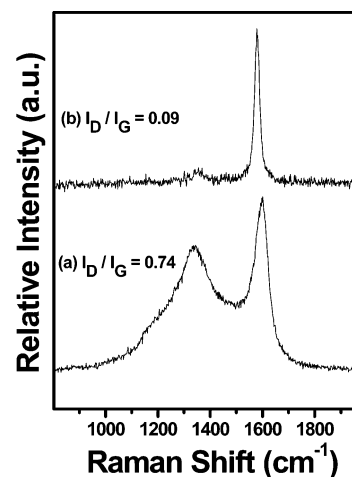


**Figure 3.** Raman spectra of (a) the as-obtained necklace-like hollow CNSs by the reaction of ferrocene [ $Fe(C_5H_5)_2$ ] and hexachlorocyclopentadiene ( $C_5Cl_6$ ) and (b) the solid chainlike carbon spheres by the reaction of naphthalene ( $C_{10}H_8$ ) and hexachlorobenzene ( $C_6Cl_6$ ).

spectroscopy was also applied to the as-prepared necklace-like hollow CNSs. As shown in Figure 3a, the G band at  $1597\text{ cm}^{-1}$  corresponds to an  $E_{2g}$  mode of graphite, while the D band at around  $1344\text{ cm}^{-1}$  is associated with vibrations of carbon atoms with dangling bonds in plane terminations of disordered graphite or glassy carbon.<sup>15</sup> Thus, the relative intensity ratio of  $I_D$  and  $I_G$  was regarded as a usual measurement for the graphitic ordering: the greater the ratio of  $I_D$  and  $I_G$ , the higher the disorder degree for graphite.<sup>16</sup> In this case, the value of  $I_D/I_G$  of the necklace-like hollow CNS sample obtained by the reaction of two pentagonal units [ $Fe(C_5H_5)_2$  and  $C_5Cl_6$ ] is 0.74, which is much greater than the value for highly graphited carbon,<sup>17</sup> indicating the defect-exist lattice disordering. As a comparison, the value of  $I_D/I_G$  for the carbon materials obtained by two hexagon-unit reactants is 0.09, as shown in Figure 3b, suggesting that the relatively highly ordered graphite carbon can be obtained by the construction of hexagonal units. This result also reveals that the multiwalls forming hollow spheres have a lattice with plane termination, edges, and defects, which may be related to the existence of a pentagon in the final products arising from the additives of pentagon units in the reaction process.

The disordering character is also reflected by the corresponding XRD patterns; the as-obtained necklace-like hollow CNSs show no sharp peaks in the full XRD range (Figure 4a). However, as for the solid carbon spheres obtained by hexagon-unit reactants, the XRD pattern is highly crystalline and all of the peaks can be indexed to graphite (JCPDS Card Files, No. 41-1487), as shown in Figure 4b. This result suggests that the carbon materials obtained by the hexagon-unit reactants show a high degree of long-range order, while the hollow CNSs obtained by the pentagon-unit reactants have a lower degree of long-range order from the crystal-

(13) (a) Calderon-Moreno, J. M.; Yoshimura, M. *J. Am. Chem. Soc.* **2001**, *123*, 741–742. (b) Tuinstra, F.; Koenig, J. L. *J. Chem. Phys.* **1970**, *53*, 1126–1130.

(14) Klinke, C.; Kurt, R.; Bonard, J. M.; Kern, K. *J. Phys. Chem. B* **2002**, *106*, 11191–11195.

(15) Dresselhaus, M. S.; Dresselhaus, G.; Pimenta, M. A.; Eklund, P. C. In *Analytical Applications of Raman Spectroscopy*; Pelletier, M. J., Ed.; Blackwell Science: Oxford, U.K., 1999; Chapter 9.

(16) Niwase, K.; Homae, T.; Nakamura, K. G.; Kondo, K. *Chem. Phys. Lett.* **2002**, *362*, 47–50.

(17) Kasuya, A.; Sasaki, Y. *Phys. Rev. Lett.* **1997**, *78*, 4434–4437.

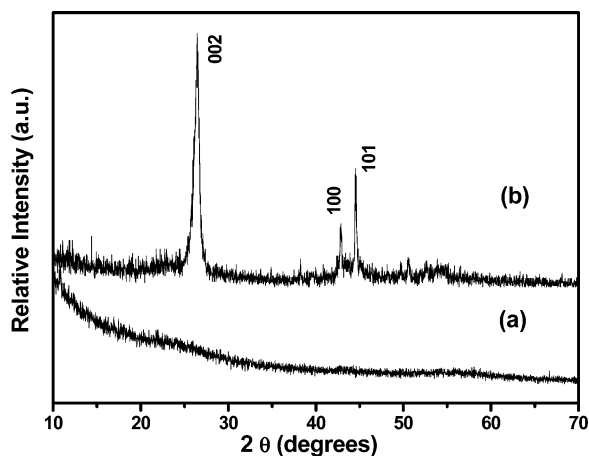


**Figure 4.** XRD patterns of (a) the as-obtained necklace-like hollow CNSs by the reaction of ferrocene [ $\text{Fe}(\text{C}_5\text{H}_5)_2$ ] and hexachlorocyclopentadiene ( $\text{C}_5\text{Cl}_6$ ) and (b) the solid chainlike carbon spheres by the reaction of naphthalene ( $\text{C}_{10}\text{H}_8$ ) and hexachlorobenzene ( $\text{C}_6\text{Cl}_6$ ).

lography point of view, which may be related to the incorporation of pentagons in the graphited carbon and thus destroy the crystallographic periodicity for a two-dimensional lattice.

**3.3. Study of the Reaction Mechanism by Comparison Experiments.** Efforts have been made to rationalize the formation process of necklace-like hollow CNSs. The experimental results suggest that the growth mechanism of the necklace-like hollow CNSs in the present work is different from that in early reports that the transition-metal particles<sup>18</sup> and the simple rolling of a hexagonal lattice of  $\text{sp}^2$ -bonded graphite sheets<sup>5</sup> was responsible for the nucleation and growth of hollow carbon spheres because of the lack of a metal cap at the end of the necklace and the absence of large sheets coexisting with the nanonecklaces, respectively. For our present case, necklace-like hollow CNSs possibly come into being from synergic action by five-membered cyclic reactants and the produced gas as a template in the reaction process based on the analysis of the comparison experiments, which are summarized in Table 1.

First, the generation of gaseous HCl in the reaction process may also favor the formation of hollow carbon spheres. The following comparison experiments provide auxiliary evidence of the important template role of gaseous HCl: Reacting  $\text{C}_5\text{Cl}_6$  with magnesium instead of ferrocene resulted in the formation of chainlike solid particles with the average diameters of 80–90 nm and lengths of several micrometers, as shown in Figure 5a, rather than hollow nanospheres. A similar phenomenon is also found in the carbon product by the reaction of  $\text{C}_5\text{Cl}_6$  and K, which consists of chainlike solid particles with an average diameter of 60 nm in large scale (Figure 5b). That is to say, the reaction of five-membered cyclic units of  $\text{C}_5\text{Cl}_6$  with alkali metal and alkaline earth metal, as dechlorinate reactants, produced solid carbon nanostructures with the existence of the ionic salts KCl and  $\text{MgCl}_2$  as byproducts, while there was no HCl produced in

the reaction process. Additionally, without the gaseous HCl produced in the combination reaction, direct pyrolysis of  $\text{C}_5\text{Cl}_6$  or ferrocene at 500 °C only leads to the formation of carbon solid particles rather than hollow structures. Shown in Figure 5d,e are the typical images for pyrolysis of  $\text{C}_5\text{Cl}_6$  and ferrocene, respectively, further confirming the essentiality of gaseous HCl produced in the combination reaction as the template for the formation of hollow spheres.

It is found that the participation of five-membered cyclic reactants is also indispensable to the formation of necklace-like hollow CNSs. From a theoretical point of view, a structure model based on the necklace-like hollow CNSs, which is assumed to be composed of the regular occurrence of nonhexagonal rings at the atomic level, instead of regular graphene layers.<sup>19</sup> In this regard, the results of comparison experiments were consistent with the theoretical structure analysis. As shown in Figure 5c, when the six-membered cyclic reactant of hexachlorobenzene was introduced instead of one of the five-membered reactants ( $\text{C}_5\text{Cl}_6$ ), the final products only include lamellar sheets with curling morphology.

In a word, on the basis of the above considerations, the formation of necklace-like carbon nanostructures is caused by synergic action by five-membered cyclic reactants and the in situ generated HCl gas in the reaction process. Evidently, the formation process for hollow CNSs results from the construction of carbon atoms with the existence of a large number of pentagon defects occurring on the perisphere of the HCl gas template. Despite this, especially, this fact provides an example for the synthesis of hollow spheres built from nonhexagonal defects taking pentagon units as an example, which is a necessary support for the previous theoretical prediction.<sup>7</sup>

Additionally, it is obvious that the reaction temperature played a critical role in the formation of hollow carbon spheres. When the reaction temperature was lower than 300 °C, the reaction could not be initiated. Within the reaction temperature range of 450–550 °C, large quantity of necklace-like hollow CNSs could be observed in the as-synthesized sample, as shown in Figure 3. At 600 °C for 8 h, many vessels appeared in the as-synthesized product, as shown in Figure 2b, indicating that the reaction temperature is vital for the control of the nanostructures, perhaps because of the fact that hollow spheres have less surface strain and need less energy to form.

**3.4. Electrochemical Hydrogen Storage Behavior of As-Synthesized Necklace-Like Hollow CNSs.** As for the development of a new generation of hydrogen storage materials, the electrochemical hydrogen storage performance of hollow CNSs (as one kind of morphology catalog) was lacking possibly because of the difficulty in the large-scale synthesis of hollow nanospheres so far.<sup>5</sup> As is known, hollow carbon spheres usually possess a thin wall and a hollow inside and also have the potential of providing an ideal pore structure fit for hydrogen storage similar to that of MWCNTs.<sup>10</sup>

(18) Okuno, H.; Grivei, E.; Fabry, F.; Gruenberger, T. M.; Gonzalez-Aguilar, J.; Palnichenko, A.; Fulcheri, L.; Probst, N.; Charlier, J. C. *Carbon* **2004**, *42*, 2543–2549.

(19) Biro, L. P.; Mark, G. I.; Horvath, Z. E.; Kertesz, K.; Gyulai, J.; Nagy, J.; Lambin, P. *Carbon* **2004**, *42*, 2561–2566.

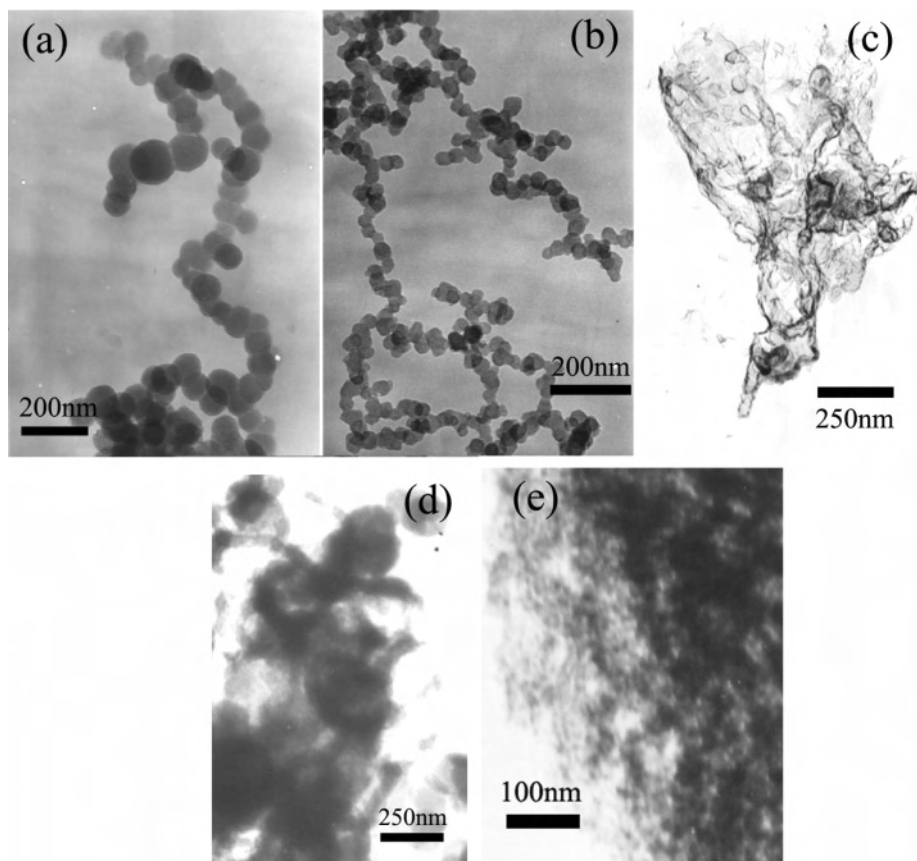


**Figure 5.** TEM images of the products for the as-prepared carbon materials obtained by the reaction of  $C_5Cl_6$  and Mg (a),  $C_5Cl_6$  and K (b), and  $C_6Cl_6$  and ferrocene (c) and the direct pyrolysis of  $C_5Cl_6$  (d) and ferrocene (e).

For our mesoporous necklace-like hollow CNSs, calculated from the discharge curves in Figure 6a, the discharge capacity of the hollow spheres is ca. 242 mAh/g at the first cycle and 176 mAh/g at the 50th cycle, higher than the previously reported electrochemical capacities for the multiwalled nanotubes,<sup>10,11</sup> and the solid chainlike carbon spheres were obtained by the reaction of naphthalene ( $C_{10}H_8$ ) and hexachlorobenzene ( $C_6Cl_6$ ). Figure 6b shows the first charge and discharge curves of the solid particle electrode, the value of which is 106 mAh/g at the current density of 200 mA/g, much lower than the first discharge hydrogen storage capacity for necklace-like hollow CNSs at the same current density, indicating that the electrochemical hydrogen storage is related with the structure and morphology of carbon materials. Besides, Figure 6c shows a capacity retention rate over many cycles for a hollow CNS electrode. Even after 50 cycles, the reversible capacity retains more than 70% of the maximal capacity, indicating a well capacity retention for our hollow nanospheres.

Here, at the current density range from 50 to 500 mA/g, it is found that the hollow CNSs/Cu electrode shows no drastic changes for the discharge capacity, indicating that the electrode exhibits a good stability for different current densities. At the lower current density of 50 mA/g, the discharge capacity is ca. 241 mAh/g (S3 in the Supporting Information). Additionally, the discharge capacity of the necklace-like hollow CNSs at the relatively high current density of 500 mA/g is 256 mAh/g (S3 in the Supporting

Information), approaching the value of 242 mAh/g at the current density of 200 mA/g, suggesting that the hollow CNSs/Cu electrode can serve as not only a “high capacity anode” but also a “high power capability anode”.

In the present case, it is considered to be more favorable to hydrogen storage for as-obtained necklace-like hollow CNSs by both gas-phase adsorption and electrochemical charge/discharge. First, identifying the pore structure of adsorbents is an essential procedure for better understanding its higher electrochemical hydrogen storage capacity for the necklace-like hollow CNSs in this case. Figure 7 and its inset show representative nitrogen adsorption/desorption isotherms and the corresponding Barrett–Joyner–Halenda (BJH) pore-size distribution curve of the obtained carbon product. The nitrogen sorption isotherm of the product exhibits type IV with an H1-type hysteresis loop at high relative pressure, which means that the resultant product possesses mesoporous structures.<sup>20</sup> The pore-size distribution of nanospheres was calculated from nitrogen desorption using the BJH model, where the results show a narrow distribution centered at 5 nm. The BET surface area of hollow nanospheres was calculated from the results of nitrogen adsorption and found to be 594.32 m<sup>2</sup>/g, which is a much higher value than that of other hollow CNSs<sup>21</sup> and MWNTs (10–20 m<sup>2</sup>/g).<sup>22</sup> By

(20) Vinu, A.; Sawant, D. P.; Ariga, K.; Hartmann, M.; Halligudi, S. B. *Microporous Mesoporous Mater.* **2005**, *80*, 195–203.

(21) Wang, Y. L.; Nepal, D.; Geckeler, K. E. *J. Mater. Chem.* **2005**, *15*, 1049–1054.

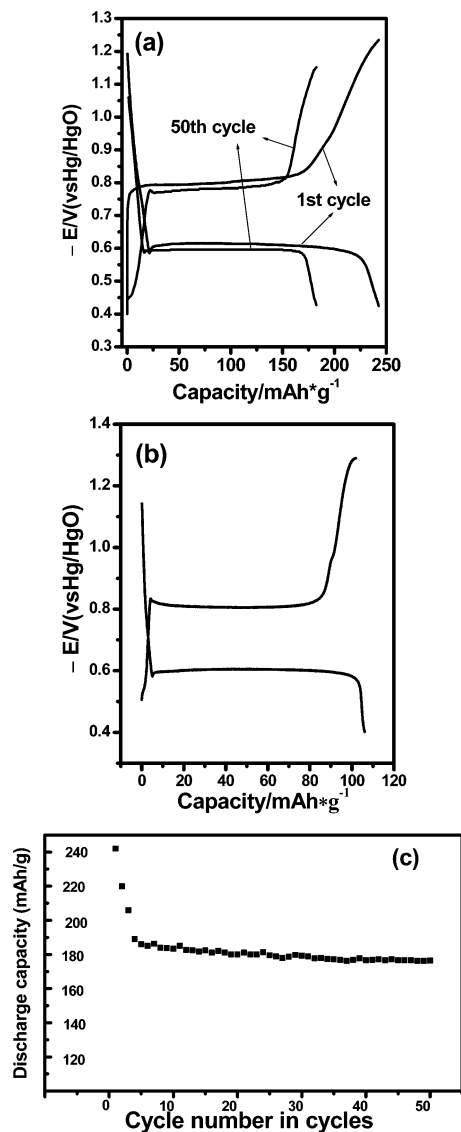
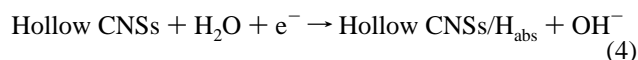


**Figure 6.** (a) Charge and discharge curves of the necklace-like hollow CNS electrode at the current density of 200 mA/g. (b) First charge and discharge curves of a solid chainlike carbon sphere electrode obtained by the reaction of naphthalene (C<sub>10</sub>H<sub>8</sub>) and hexachlorobenzene (C<sub>6</sub>Cl<sub>6</sub>) at the current density of 200 mA/g. (c) Cycle life performance of the necklace-like hollow CNS electrode at the current density of 200 mA/g.

considering that the as-obtained hollow spheres have the mesoporous structure and a high BET value, then hydrogen may be packed within the pores and hollow empty inside of the as-obtained necklace-like hollow CNSs, leading to a good hydrogen capacity. Second, on account of electrochemical hydrogen storage mechanism, the electrochemical hydrogen adsorption storage is related with the structure of the carbon materials. Here, the electrochemical hydrogen adsorption storage of carbon materials relies on the dissociation of water at the working electrode in an alkaline solution:



It is found that the H/C ratio is 0.02 and 0.03 by the elemental analysis measurement before and after the elec-

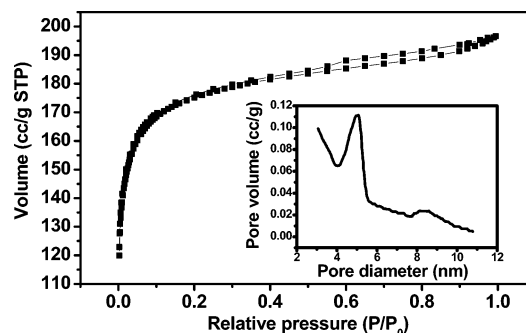


**Figure 7.** Nitrogen adsorption/desorption isotherms of the obtained mesoporous necklace-like hollow CNSs. Inset: BJH pore-size distribution curve determined from the nitrogen desorption isotherm.

trochemical cycling for 50 cycles, respectively. That is to say, the hydrogen content did not increase significantly in this case, confirming the adsorption mechanism of hydrogen. As for the electrochemical process, when the hydrogen adsorption energy is higher than the hydrogen released energy, the adsorbed hydrogen can further diffuse in the carbon host occupying sites with higher adsorption energy, which strongly depends on the size and shape of the carbon materials.<sup>23</sup> The structural characteristics of ultrathin walls and large amounts of defects will facilitate hydrogen to not only deposit between the layers of hollow carbon spheres through the diffusion process but also enter into the empty space inside hollow carbon spheres, which leads to the high hydrogen storage electrochemical capacity of hollow spheres.

**3.5. Lithium Ion Intercalation Behavior of As-Synthesized Necklace-Like Hollow CNSs.** The crystallinity, the microstructure, and the micromorphology of carbonaceous materials strongly influence the quality of sites capable of lithium accommodation.<sup>24</sup> Then the kind of carbon determines the current/potential characteristics of the electrochemical intercalation reaction, as well as the lithium ion intercalation capacity characteristics.<sup>25</sup> In this regard, the increasing surface area and disorder degree of the carbonaceous materials are expected to improve the performance for the lithium ion intercalation.<sup>26</sup> Thus, the as-obtained necklace-like hollow CNSs, which possess thin walls, hollow insides, and high BET values, also provide examples to investigate their lithium ion intercalation performances because of the possibly increased active sites for electrochemical lithium insertion/deinsertion. The voltage profile of a hollow CNSs/Li cell in the discharge curves shows the electrochemical discharge behavior with a voltage of 0.05–2.0 V. As shown in Figure 8, the irreversible capacity of necklace-like hollow CNSs (539 mAh/g) for the first cycle is significantly larger than that of solid chainlike carbon spheres (134 mAh/g). It is generally accepted that the irreversible capacity of carbonaceous materials at the first

(23) Jurewicz, K.; Frackowiak, E.; Béguin, F. *Appl. Phys. A* **2004**, *78*, 981–987.

(24) Besenhard, J. O. In *Progress in Intercalation Research*; Müller-Warmuth, W., Schöllhorn, R., Eds.; Kluwer: Dordrecht, The Netherlands, 1994; p 457.

(25) Fauteux, D.; Koksang, R. *J. Appl. Chem.* **1993**, *23*, 1.

(26) Winter, M.; Besenhard, O. J.; Spahr, M. E.; Novak, P. *Adv. Mater.* **1998**, *10*, 725.

(22) Ajayan, P. M. *Chem. Rev.* **1999**, *99*, 1787–1800.

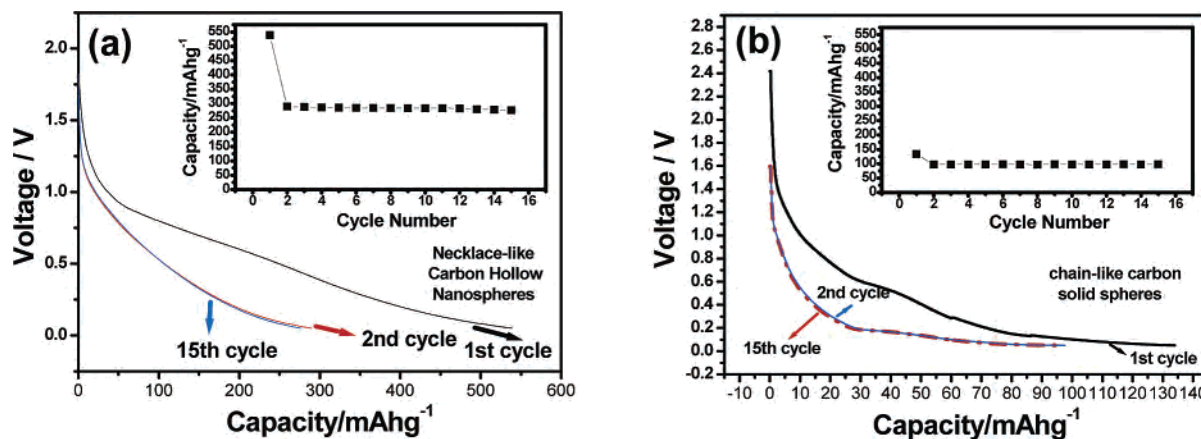


**Figure 8.** Voltage versus discharge capacity curves for (a) the necklace-like hollow CNSs/Li cell and (b) solid chainlike carbon spheres/Li cell between 2.0 and 0.05 V at the 1st, 2nd, and 15th cycles, respectively. Insets in parts a and b are the corresponding cyclic performances for the necklace-like hollow CNSs/Li and solid chainlike carbon spheres/Li cells, respectively.

cycle is largely attributed to the electrolyte instability, i.e., decomposition of the electrolyte on the electrode surface and reaction of lithium with active sites in the electrode, which are typically enhanced with increasing surface area and disorder degree in the carbonaceous materials, respectively.<sup>27</sup> Accordingly, the increase in the irreversible capacity of our hollow sample is probably due to the increased surface area and structural defects/disordered phase of necklace-like hollow CNSs as described above, compared with the solid chainlike carbon spheres. On the other hand, the reversible capacity of necklace-like hollow CNSs at the second cycle (290 mAh/g) at a constant discharge rate of 0.2 mA/cm<sup>2</sup> increased significantly as compared to that of solid chainlike spheres (97 mAh/g). This indicates that increases in the disorder degree and high BET value in the necklace-like hollow CNSs, arising from the additives of pentagon units in the reaction process, are useful to generate the active sites available for reversible lithium storage and exhibit a capacity advantage compared with those for the solid carbon spheres obtained by two hexagonal units such as C<sub>6</sub>Cl<sub>6</sub> and C<sub>10</sub>H<sub>8</sub> under the same conditions, giving us further information for the disorder degree in the necklace-like hollow CNS products. Additionally, the insets in Figure 8 show the reversible capacity of 276 mAh/g up to 15 cycles, which suggests that insertion/extraction of the lithium ion produces high reversibility and little hysteresis from the second cycle for the necklace-like hollow CNSs.

#### 4. Conclusions

In conclusion, necklace-like hollow CNSs have been successfully synthesized from the pentagon-including reac-

tants, which provide an auxiliary example for the theory prediction that necklace-like hollow CNSs are assumed to be composed of the regular occurrence of nonhexagonal rings at the atomic level. The benefits for the as-obtained hollow CNSs also arise from the high BET value of 594.32 m<sup>2</sup>/g and a narrow pore-size distribution at 5 nm. For these mesoporous necklace-like hollow CNSs, a hydrogen storage capacity of 242 mAh/g at the current density of 200 mA/g corresponding to a hydrogen storage of 0.89 wt %, which is higher than the previously reported capacities for the multiwalled nanotubes, could be achieved in the electrochemical hydrogen storage experiments. Also, the necklace-like hollow CNSs exhibit a significant capacity advantage for lithium ion intercalation compared with the solid carbon spheres obtained by two hexagonal units such as C<sub>6</sub>Cl<sub>6</sub> and C<sub>10</sub>H<sub>8</sub> under the same conditions, giving us further information for the disorder degree in the necklace-like hollow CNS products. These results indicate that the necklace-like hollow CNSs provide a new candidate for application in hydrogen storage and lithium batteries.

**Acknowledgment.** This work was financially supported by the National Natural Science Foundation of China (Grant 20321101) and the state key project of fundamental research for nanomaterials and nanostructures (Grant 2005CB623601). The authors also thank Dr. Shuangzheng Lin for helpful discussion of the formation mechanism.

**Supporting Information Available:** XPS survey spectrum for the as-obtained CNSs, IR spectrum of the as-obtained products for the as-synthesized hollow CNSs and materials after the electrochemical cycling for 50 cycles, and first charge/discharge curves of necklace-like hollow CNS electrodes. This material is available free of charge via the Internet at <http://pubs.acs.org>.

IC060827F

(27) Matusumura, Y.; Wang, S.; Mondori, J. *J. Electrochem. Soc.* **1995**, *142*, 2914.